Three-Dimensional Evaluation of Tritium Breeding Ratio, Nuclear Heating Distribution, and Neutron Wall Loading Profile for ARIES-ACT-1 (SiC/LiPb) Design

L. Mynsberge, A. Jaber, L. El-Guebaly

December 2012

UWFDM-1414

FUSION TECHNOLOGY INSTITUTE

UNIVERSITY OF WISCONSIN

MADISON WISCONSIN

Three-Dimensional Evaluation of Tritium Breeding Ratio, Nuclear Heating Distribution, and Neutron Wall Loading Profile for ARIES-ACT-1 (SiC/LiPb) Design

L. Mynsberge, A. Jaber, L. El-Guebaly

Fusion Technology Institute
University of Wisconsin
1500 Engineering Drive
Madison, WI 53706

http://fti.neep.wisc.edu

December 2012

UWFDM-1414

Abstract

The ARIES team has just completed the detailed design of ARIES-ACT-1 with aggressive physics and advanced SiC technology. Accurate neutronic characterizations of ARIES-ACT-1 are essential in determining its operational nuclear parameters. The neutron wall loading (NWL), tritium breeding ratio (TBR), and nuclear heating distribution are parameters that must be determined for tritium self-sustainability and adequate shielding and protection of ARIES fusion power plants. After determining the NWL profile at the first wall (FW), radial builds were defined to satisfy the shielding requirements. Using the DAGMC code that couples the CAD drawings with the MCNP Monte Carlo radiation transport code, the NWL, breeding, and heating parameters were determined for ARIES-ACT-1. The peak NWL values are 2.9 MW/m^2 for the inboard FW, 4.5 MW/m^2 for the outboard FW, and 1.8 MW/m^2 for the divertor. The degradation of the tritium breeding based on the addition of individual design elements to the 3-D model calculated a final TBR of 1.05. Analysis of the nuclear heating determined the energy multiplication to be 1.144. Our final 3-D nuclear analyses had much to do with defining and reshaping the radial and vertical builds of ARIES-ACT-1.

I. Introduction

The ARIES team [1] is currently developing four power plants that are designed with a range of aggressive and conservative tokamaks (ACT). Four ARIES-ACT designs proceeded interactively while the systems code determined the reference parameters through varying the physics and engineering parameters to produce an economic optimum for each design:

- Aggressive physics with SiC-based blanket (ARIES-ACT-1)
- Conservative physics with ferritic steel-based blanket (ARIES-ACT-2).
- Aggressive physics with ferritic steel-based blanket (ARIES-ACT-3)
- Conservative physics with SiC-based blanket (ARIES-ACT-4).

Three-dimensional neutronic simulations of ARIES-ACT are necessary to satisfy the shielding requirements and tritium self-sufficiency. The nuclear parameters that are evaluated in this report are the neutron wall loading (NWL), tritium breeding ratio (TBR) and the nuclear heating distribution for an interim ARIES-ACT-1 design, shown in Figure 1, with a major radius of 5.5 m, minor radius of 1.375 m, and fusion power of 1804 MW. The NWL is a fusion power normalized neutron current density at the FW. It enables the design of adequately defined radial and vertical builds and ensures proper shielding against the high-energy fusion neutrons. The TBR is a measure of how many tritium atoms are created from nuclear reactions with lithium within the blanket per tritium atom consumed by the plasma. The nuclear energy multiplication is a measure of the energy deposited by neutrons and photons in the various high-temperature in-vessel components per neutron energy from the plasma.

ARIES-ACT-1 employs the SiC/SiC composite structure with the LiPb tritium breeder, much like the ARIES-AT design [2,3]. The LiPb serves in a configuration that allows not only breeding but also self-cooling of the blanket SiC structure. The SiC FW serves to protect the blankets from high radiant heat and particle fluxes from the plasma. The ARIES-ACT-1 design requires the calculated TBR to be 1.05 [4] to account for deficiencies and uncertainties. Generally, the margin for the calculated TBR (calculated TBR–1) arises from known deficiencies in nuclear data, known deficiencies in modeling, unknown uncertainties in design elements, and tritium bred in excess of the tritium consumed by D-T fusion reactions within the plasma [5]. For ARIES-ACT, the margin totals to approximately 5%.

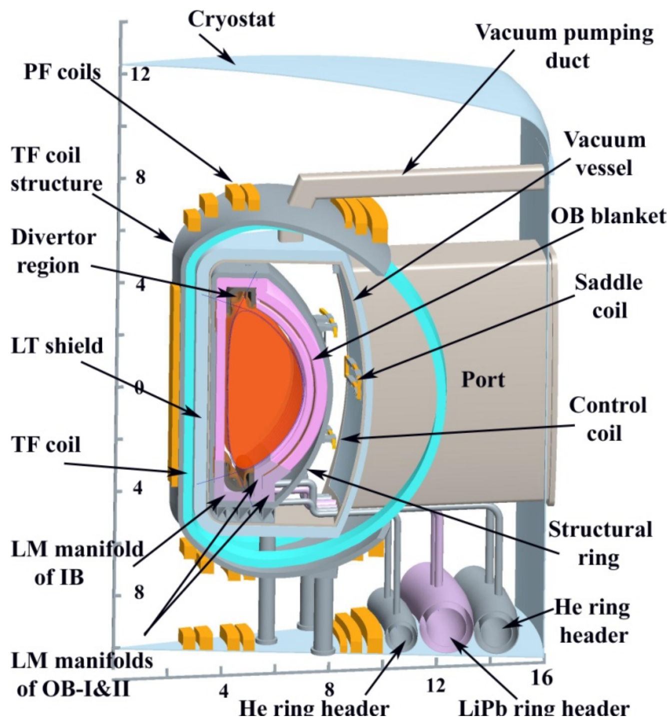

Fig. 1. Isometric view of ARIES-ACT-1.

II. Methodology and Codes

A coupling of computer codes was used to perform the neutronic analysis for the ARIES-ACT-1 design. These codes were Cubit and Directly Accelerated Geometry Monte Carlo (DAGMC). Cubit was used for the solid modeling needed to build the model to be used by DAGMC for performing the Monte Carlo radiation transport. The DAGMC code was used for the Monte Carlo simulations since it allowed neutron transport directly on a computer-aided design (CAD) model, which is incredibly useful for such 3-D geometries.

Cubit is a solid modeling and mesh generation software toolkit developed and released by Sandia National Laboratories [6]. Cubit provided the ability to build and prepare 3-D models necessary for CAD-based radiation transport to be used for the 3-D analysis. Cubit was required for its unique ability to detect and eliminate redundant surfaces of adjacent volumes through the use of the imprint and merge functions. Inadequate designs will cause incomplete imprinting and merging that will result in a poorly defined geometry and lost particles in the radiation transport simulation. Cubit not only gives the user the ability to create the complete 3-D geometry, but it also can group volumes and surfaces in order to assign material densities, define boundary conditions, and define desired tallies for the radiation transport simulation. Cubit provided the ability to build the model to be used by the next code, DAGMC, to perform the Monte Carlo radiation transport.

The DAGMC code [7] is a software tool developed by the Computational Nuclear Engineering Research Group (CNERG) at the University of Wisconsin-Madison that provides the ability to perform Monte Carlo radiation transport on 3-D geometries created by solid modeling software. This code gives the ability to translate a CAD model into a faceted 3-D geometry that can be interpreted by radiation transport software. DAGMC utilizes the radiation transport code MCNP5 [8]. By using Cubit to prepare the geometry, the user is only required to create a portion of the data cards associated with a typical MCNP5 input. The nuclear data used in this analysis is taken from Fusion Evaluated Nuclear Data Library [9].

ARIES-ACT-1 is modeled as the upper half of an 11.25^{o} wedge throughout the 3-D analysis. There are 16 blanket modules that span 22.5^{o} each, thus the 11.25^{o} wedge in the CAD model represented one half of a complete blanket module. Reflecting surfaces were placed on both sides of the 11.25^{o} wedge as well as at the midplane. Thus, the 3-D model represented $1/64^{th}$ of the complete tokamak. The neutron source distribution within the plasma region was approximated using a three-nested source distribution with varying intensities (63%, 32%, and 5%) [10].

The most innovative feature of this analysis is the assessment of the degradation of individual design elements to the TBR of the ARIES-ACT-1 blanket design. There were 8 individual simulations that measured the impact of design elements, including curvature of blanket walls, W stabilizing shell, and assembly gaps between blanket modules. The impact of varying the enrichment was determined and the reduction in TBR due to penetrations was estimated.

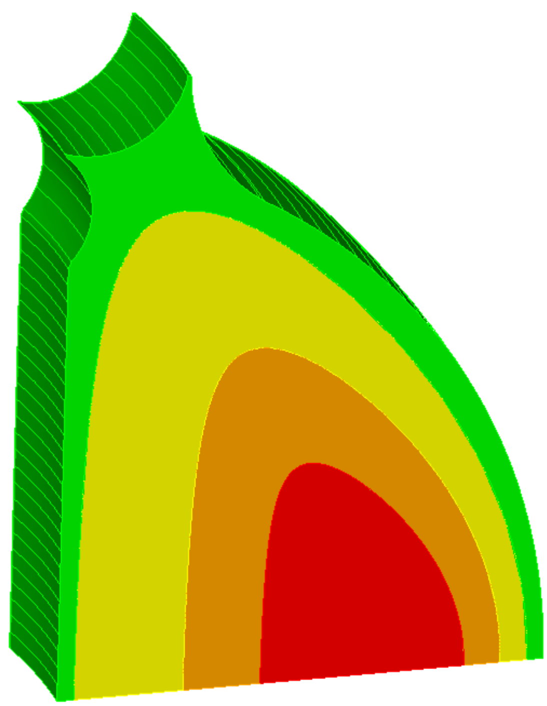

Fig. 2. 3-D ARIES-ACT-1 model used for the NWL analysis. The FW surfaces are segmented in order to accurately obtain the NWL at various surfaces.

III. Neutron Wall Loading Results

Using Cubit to build and prepare a 3-D model in addition to DAGMC to perform Monte Carlo radiation transport on the model, neutronic simulations were performed to obtain the NWL distribution along the FW of ARIES-ACT-1. Figure 2 shows the 3-D model that was used for the analysis.

III-a. Inboard and Outboard First Walls

Results shown in Figure 3 were obtained for the NWL distribution along the inboard (IB) and outboard (OB) FW of an interim ARIES-ACT-1 design with a major radius of 5.5 m, minor radius of 1.375 m, and fusion power of 1804 MW. The NWL decreased as the vertical distance from the midplane increased. The peak NWL occurred at the midplane for the IB and OB FW. The IB peak NWL is 2.9 MW/m^2 and the OB peak is 4.5 MW/m^2.

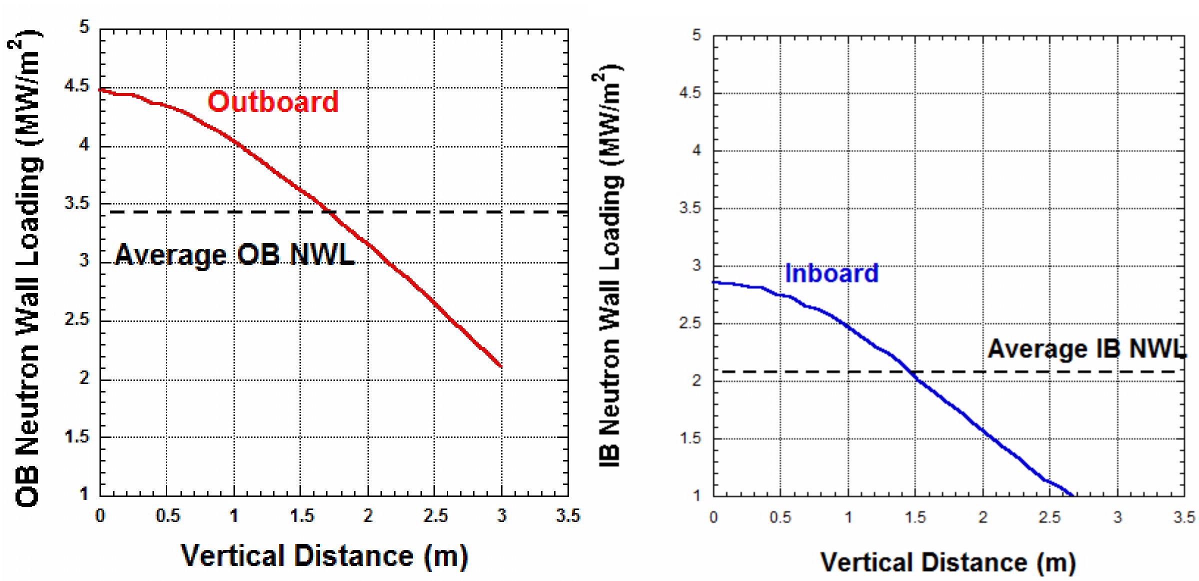

Fig. 3. IB and OB FW NWL results. The IB peak NWL is 2.8 MW/m^2 and the OB peak is 4.5 MW/m^2.

III-b. Divertor Plates

The divertor plates were segmented in order to obtain the NWL distribution along each plate. This is shown in Figure 4. As the distance from the plasma increased, the NWL decreased. As mentioned, the NWL is a measurement of current density, meaning that the angle with which the surface faces the plasma will have higher NWL. Therefore, the maximum NWL value will not necessarily occur at the lowest point for the divertor as it did with the IB and OB FW. The divertor peak NWL value of 1.8 MW/m^2 occurred near the bottom of the outer plate at a height of 3.1 m from the midplane. Figure 5 reveals the NWL distribution along each plate of the divertor. The dome plate is measured in radial distance from the center axis of the tokamak.

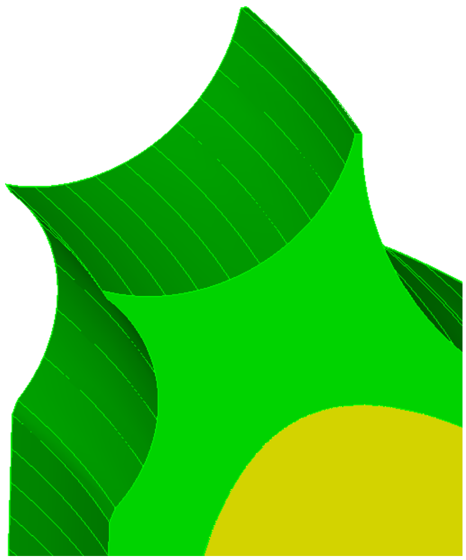

Fig. 4. The divertor area of the 3-D ARIES-ACT-1 model used for the NWL analysis. These divertor surfaces are segmented in order to accurately obtain the NWL at various surfaces.

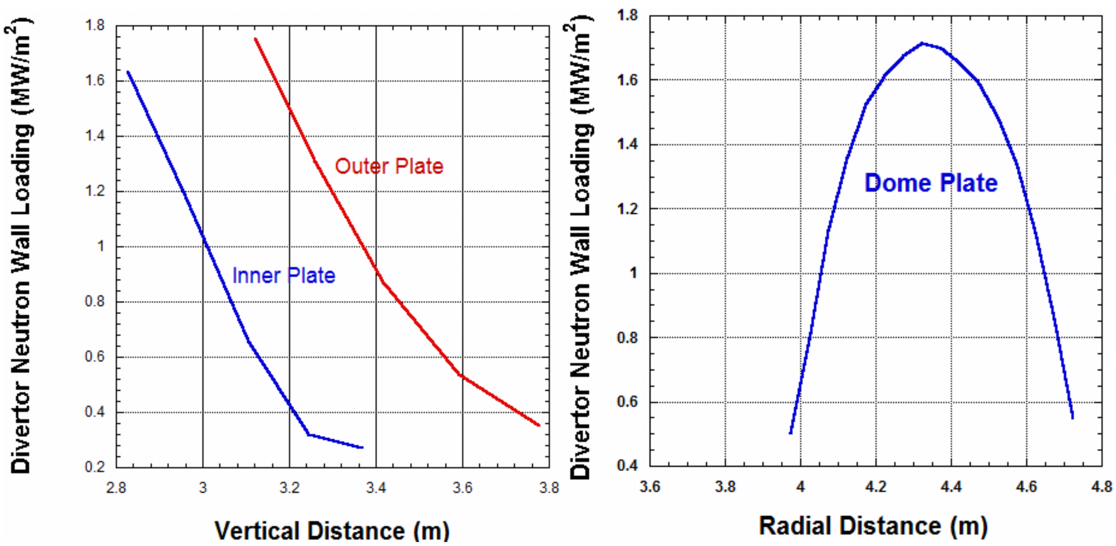

Fig. 5. Divertor NWL results. The peak NWL is 1.8 MW/m^2 and occurred near the middle of the dome plate at 3.1 m from the midplane.

III-c. Summary

To assess the key NWL parameters of the ARIES-ACT-1 design, it is pertinent to know the peak NWL values and it is also very useful to have other data such as averages. Table 1, below, summarizes all the data for the IB FW, OB FW, and the three plates of the divertor region—inner, outer, and dome.

Table 1. Neutron Wall Loading Summary

(MW/m^2)	Peak	Average
IB FW	2.86	2.08
OB FW	4.47	3.43
Divertor	1.75	1.04
Inner Plate	1.63	--
Outer Plate	1.75	--
Dome Plate	1.72	--

IV. Tritium Breeding Ratio Results

A detailed analysis of the TBR of ARIES-ACT-1 was performed to determine the impact of various design elements involved in creating the accurate and detailed 3-D blanket model. Homogenization was avoided except in the 2-3 cm thick FW, side/top/back walls, and cooling channels within the blanket. The fine structures within these components will not affect the breeding. The vacuum vessel and magnets shown in Fig. 1 were not included in the model since their impact on the TBR is insignificant. The starting ^{6}Li enrichment is 90% as in ARIES-AT as well as in past fusion studies employing LiPb as a breeder. The bottom-line results are displayed in Fig. 5 for the reference LiPb eutectic that contains 15.7 at% Li and 84.3 at% Pb [11]. This bar chart represents the calculated TBR from a series of eight 3-D runs performed to illustrate the stepwise degradation in breeding by various elements of blanket internals and surroundings. The eight individual steps are discussed below along with the detailed change(s) made to the 3-D models for each step.

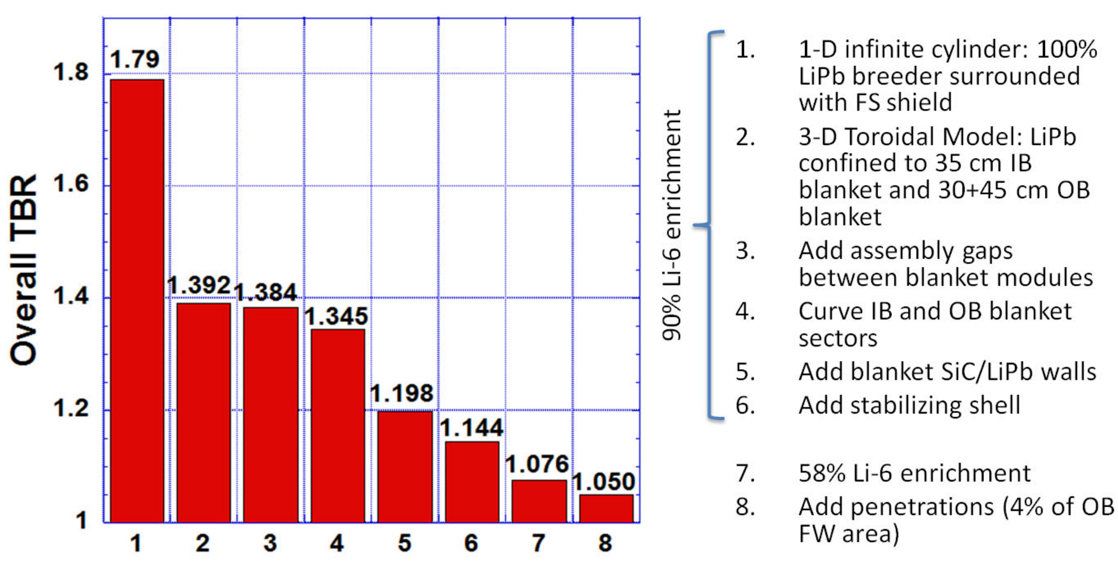

Fig. 6. This bar chart shows the reduction in TBR from 1.79 to 1.05 as a result of including the blanket details of the ARIES-ACT-1 SiC/LiPb model.

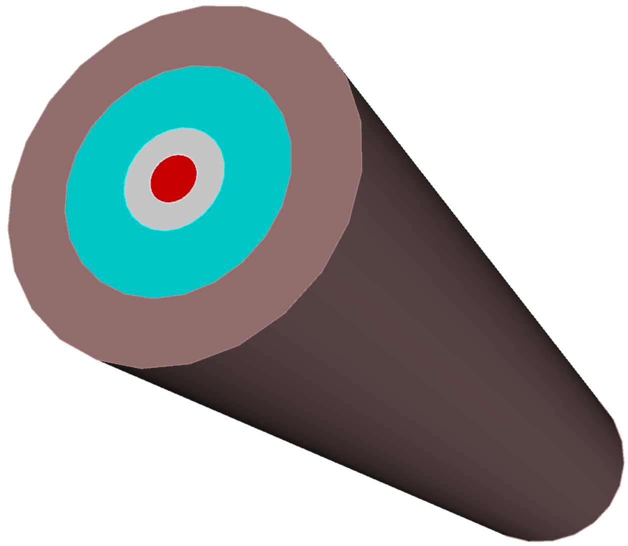

Fig. 7. Cylindrical model used to test the upper limit of breeding when using LiPb. This is an upper limit of the TBR and the first step used in the analysis. The TBR is 1.79.

IV-a. Step 1: Shielded 1-D Infinite Cylinder

In order to estimate the highest achievable TBR, a model of a 1-D infinite cylinder was created. The model consisted of a central neutron source represented by a cylinder of radius 75 cm surrounded by 85 cm void, 200 cm of $Li_{15.7}Pb_{84.3}$ breeder region, and 200 cm ferritic steel (FS) shield. Figure 7 illustrates the cylindrical model. The LiPb contains 90% enriched ^{6}Li. The top and bottom surfaces of the cylinder were assigned to be reflecting boundaries in order to model an infinite cylinder. The TBR was calculated to be 1.79 and was used as the initial reference point in the 3-D analysis as seen in Figure 6.

IV-b. Step 2: $Li_{15.7}Pb_{84.3}$ Confined to Blanket

The next step in the TBR analysis was to confine the breeder to IB and OB blankets. The IB blanket was set to be 35 cm thick and the OB blanket was a total of 75 cm thick with 2 segments consisting of 30 cm (OB-I) and 45 cm (OB-II) thick segments. Materials were assigned to the surrounding outer shield, divertor plates, and divertor shield. The outer shield was 50 cm thick on the IB, OB and top/bottom. The divertor plates are 7.7 cm thick followed by 15 cm thick support structure. Figure 8 is a schematic of the IB and OB radial builds.

The outer shield and divertor shield were given a composition of 80% ODSFS and 20% He. The divertor plates were given a composition of 8% W, 28% W-TiC, 11% ODSFS, and 53% He. Figure 9 shows the 3-D model used for this analysis. The TBR reduced to 1.392 due to confining the IB and OB blankets radially and vertically.

IV-c. Step 3: Adding Assembly Gaps

Following the confinement of the breeder to the blanket regions, a 2 cm radial-poloidal gap was modeled on one side of the 11.25^{o} ARIES-ACT wedge. The gap is a necessary design

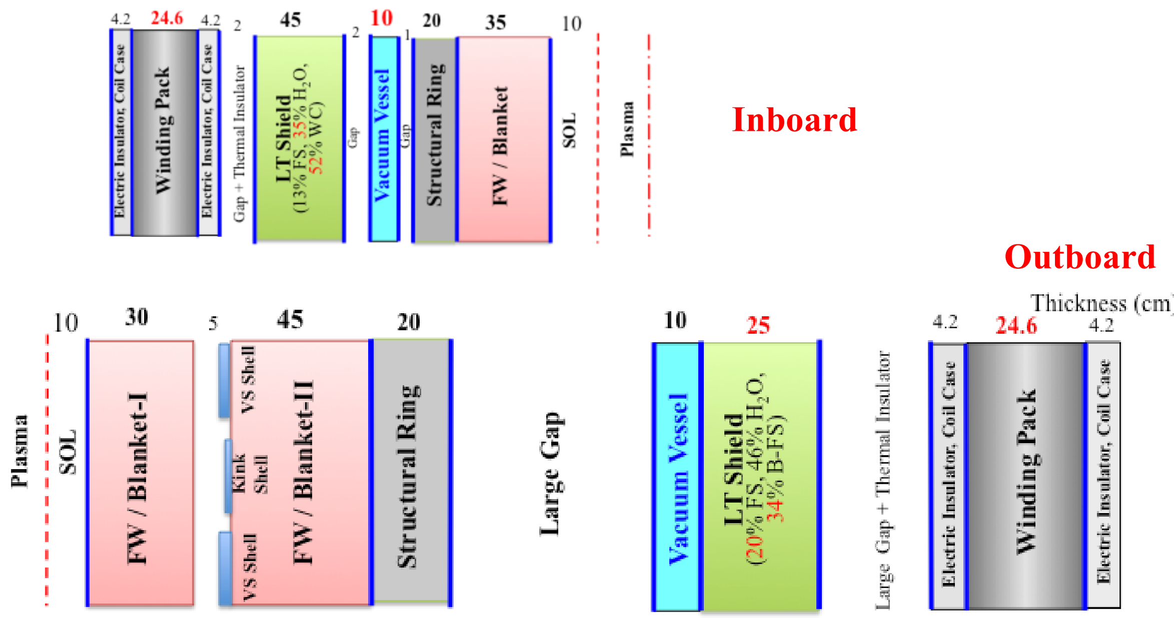

Fig. 8. This figure shows a schematic of the IB and OB radial build.

element between adjacent blanket modules to allow for thermal expansion, neutron induced swelling and the removal of blanket modules during maintenance. Figure 10 shows the gap included in the model colored in red. Since half of the blanket module is being modeled, the gap in Figure 10 is 1 cm wide. The TBR degrades slightly to 1.384 with the addition of the assembly gap.

IV-d. Step 4: Segment Blankets and Curve FW and BW

Next, the blankets were segmented into sectors and the front walls and back walls were curved. The IB has four sectors and OB-I and OB-II both have six sectors. Figure 11 shows the segmenting and curving. All other design elements maintain the same material definition as in the previous step. This caused the TBR to drop to 1.345.

IV-e. Step 5: SiC/LiPb Materials Assigned to Walls

Each of the sectors has SiC/LiPb material to contain the LiPb that will degrade the TBR, and the next step was to include these blanket walls for each sector. The thickness of the blanket walls and their composition is detailed in Table 2. Figure 12 shows a midplane cross section of the IB and OB blanket with the blanket walls defined and colored in dark blue. The TBR drops to 1.198 with the addition of the blanket walls.

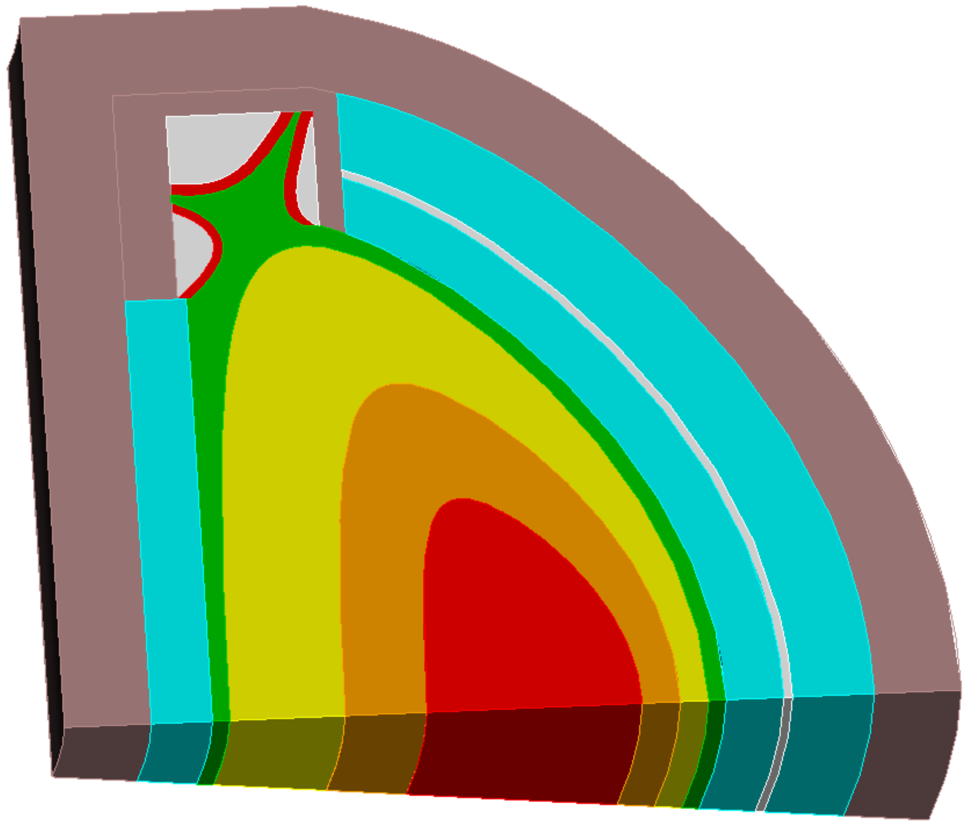

Fig. 9. 3-D CAD model of the ARIES-ACT tokamak used in determining the TBR. The breeder is confined to the blankets shown in light blue. The thicknesses at the midplane of the blanket region are 35 cm on the IB and 30 cm and 45 cm for the OB-I and OB-II blanket segments, respectively. The divertor plates are colored red. The outer shield is colored light brown. The divertor shield is also light brown.

Table 2. Blanket Wall Thicknesses

	IB Blanket (cm)	OB Blanket I (cm)	OB Blanket II (cm)
Side Wall	3.5	3.5	3.0
Top Wall	3.5	3.5	3.0
First/Front Wall	3.8	3.8	3.0
Back Wall	3.0	3.0	3.0
Compositions			
Side Wall	72.3% SiC 27.7% LiPb	72.5% SiC 27.5% LiPb	57.7% SiC, 42.3% LiPb
First/Front Wall	72.2% SiC, 27.8% LiPb	72.1% SiC, 27.9% LiPb	57.4% SiC, 42.6% LiPb
Back Wall	74.7% SiC, 25.3% LiPb	74.1% SiC, 25.9% LiPb	57.3% SiC, 42.7% LiPb
IB/OB-s Wall	86.6% SiC, 13.4% LiPb	86.6% SiC, 13.4% LiPb	51% SiC, 49% LiPb
OBII-s Outer Side Wall	--	--	67% SiC, 33% LiPb

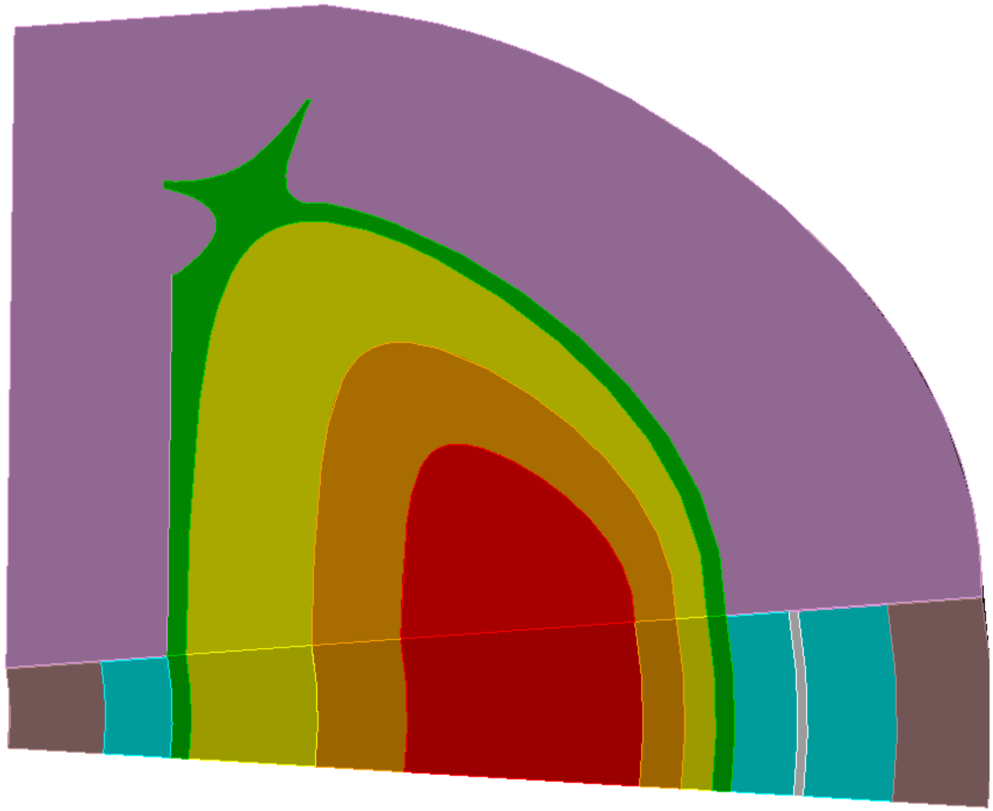

Fig. 10. This figure shows the addition of the assembly gap into the 3D model. The assembly gap is colored purple and extends over all components. The plasma region remains continuous toroidally.

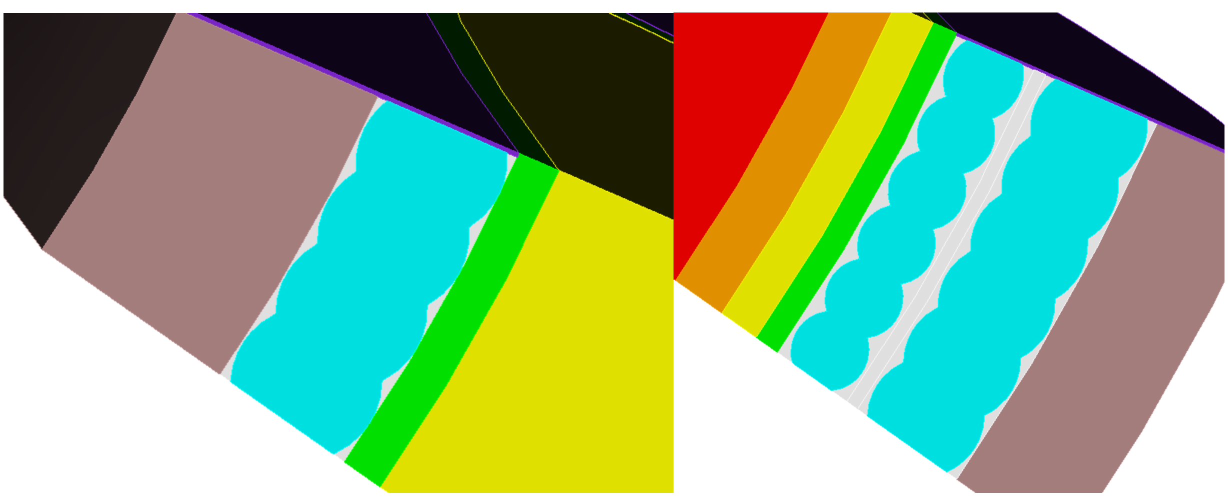

Fig. 11. A midplane view of the segmenting and curving of the sectors.

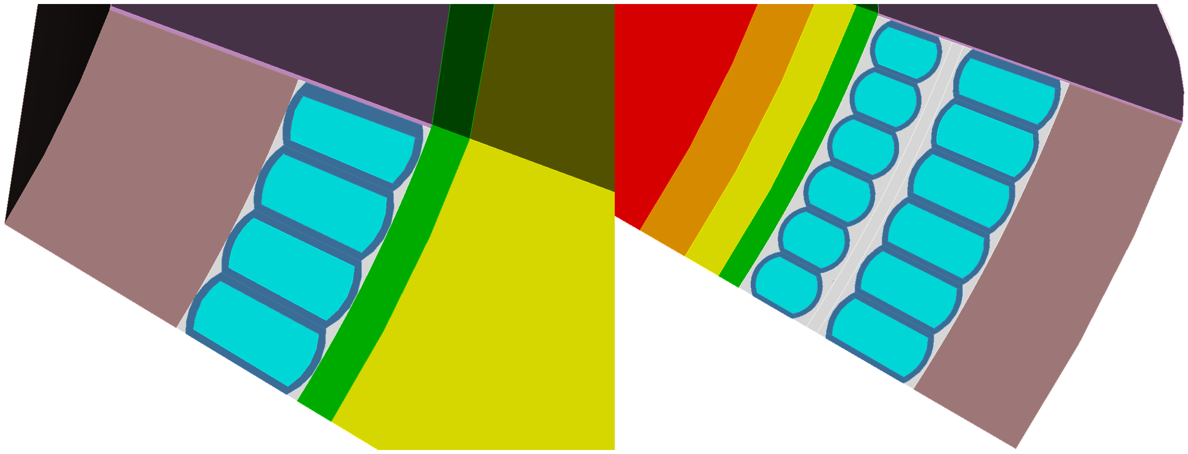

Fig. 12. Midplane cross section showing the addition of the SiC/LiPb walls. They are shown in dark blue.

IV-f. Step 6: W Stabilizing Shells Added

The TBR degradation due to the addition of the W stabilizing shells was also determined. The W shell was placed at strategic locations behind the IB blanket and between the two OB blanket segments. The IB vertical stabilizing (VS) shell was 4 cm thick and was placed between 45º and 55º with respect to the center of the major radius at 5.5 m from the machine center line. The OB VS shell was 4 cm thick and was placed between 55º and 80º with respect to the center of the major radius (1.76-2.81 m on the z-axis). And finally the OB Kink shell was 1 cm thick and placed between 0 and 45º with respect to the center of the major radius (0-1.42 m on the z-axis). The OB plates of the W shell were placed in the 5 cm gap between the OB blankets. The shells are composed of 100% W-TiC and radiate their heat to the surrounding blanket and structural ring (SR). The W shells are shown in Figure 13. The TBR is reduced to 1.144 due to the addition of the shells.

IV-g. Step 7: Varying Li-6 Enrichment

The enrichment of the ^{6}Li in the LiPb breeder was varied to determine if it is possible to operate ARIES-ACT-1 at lower enrichments. Several enrichments were used to evaluate the trend. The TBR trend due to varying the ^{6}Li enrichment is shown in Figure 14. The TBR degradation due to lower enrichment was calculated in this step. The TBR was reduced to 1.076 with 58% ^{6}Li enrichment.

IV-h. Step 8: Adding Penetrations

Finally, OB penetrations for diagnostics and plasma control were considered. The expected OB penetration FW area was 7.0 m^2. The total OB FW area was 313 m^2. This is 2.24% of the OB surface area, but to be conservative up to 4% penetrations of the OB FW was considered. The penetration area was converted to a fraction of the total FW area and multiplied by the OB contribution to the TBR. This yielded an approximate degradation of the TBR due to the addition of the penetrations in the ARIES-ACT design. The TBR decreased to 1.050 in this step. Overall, the IB and OB blankets provide 20% and 80% of the breeding, respectively. As

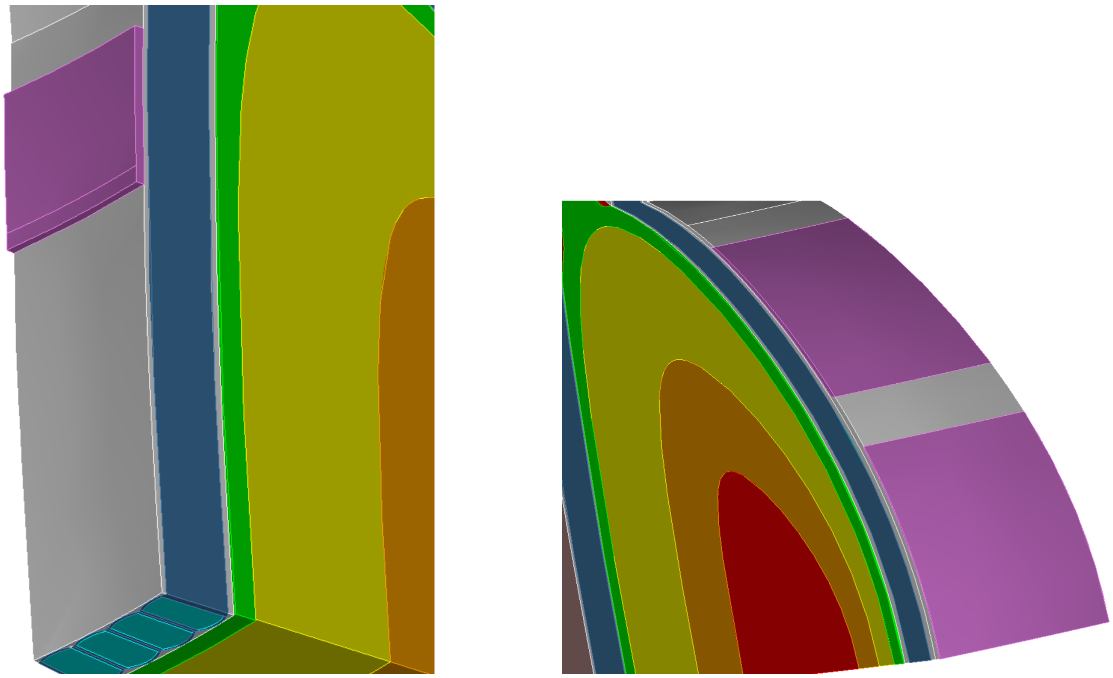

Fig. 13. This figure shows the addition of the W stabilizing shells to the inboard (left) and the outboard (right). They are colored in purple.

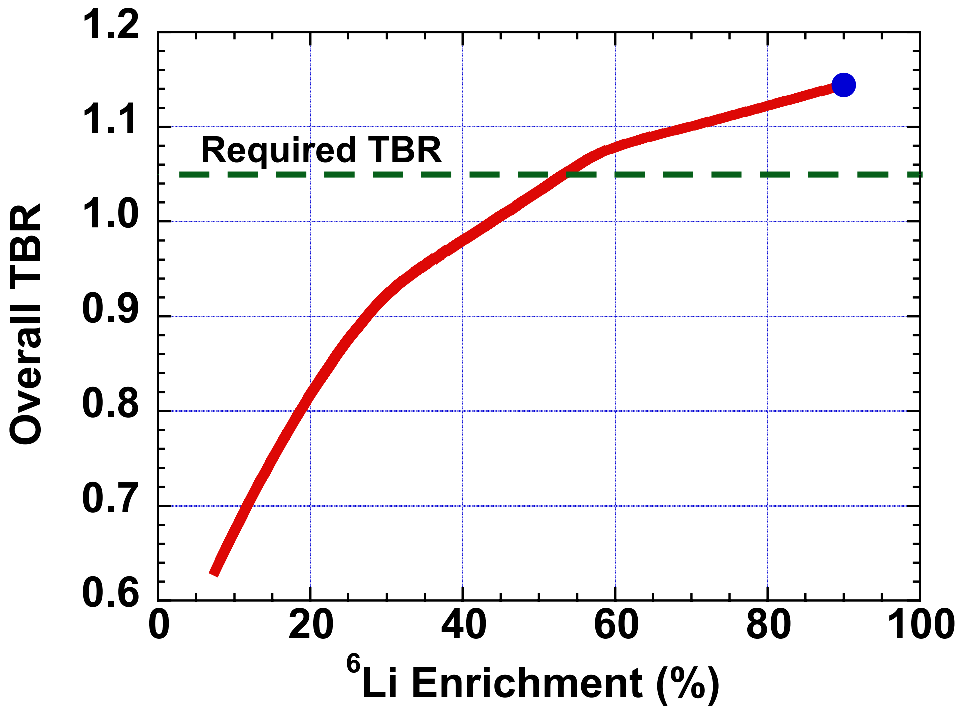

Fig. 14. Change in TBR of the extended blanket design with varying ^{6}Li enrichment within the LiPb breeder.

mentioned in the next section, the final design calls for a thicker IB blanket (45 cm) extended upward/downward, LiPb manifolds behind the divertor system, and a wider divertor slot. Such changes augment the TBR, allowing operation with a lower ^{6}Li enrichment of ~50%.

V. Nuclear Heating Distribution Results

Breaking down the ARIES-ACT-1 into individual sections allowed for a complete nuclear heating analysis. The value of heating in each section was used to obtain details on the thermal hydraulic analysis and eventually the kind of thermomechanical stresses the device is subjected to during operation. The total fusion power used in this analysis is 1804 MW.

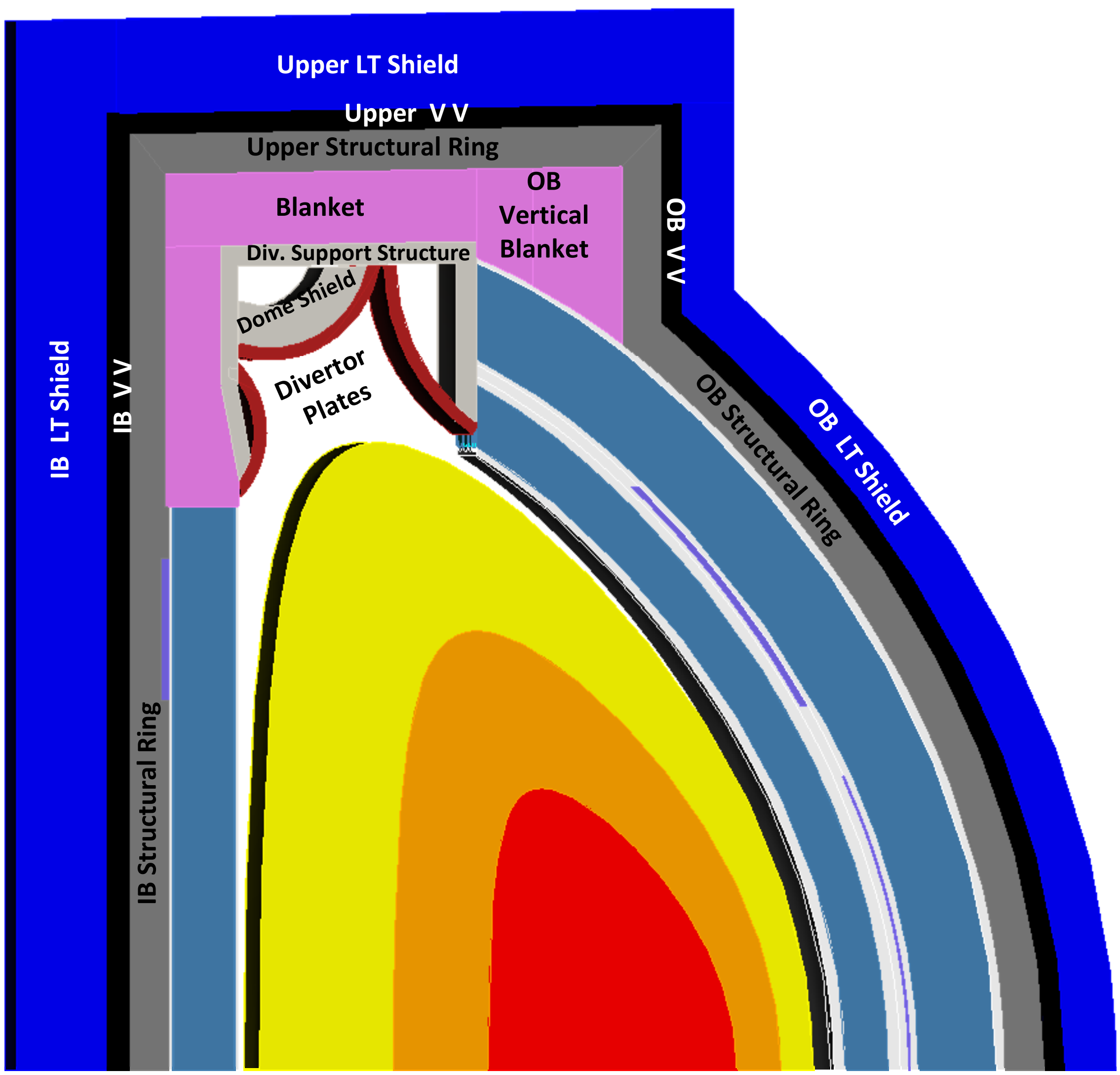

Fig. 15. Model of the upper half of the ARIES-ACT-1 design. The difference in the divertor region can be seen. The flat blanket above the divertor varies between this model and Figure 16.

V-a. Heating Model

For the nuclear heating analysis, a variant on the TBR model was used. The heating model reflects the latest changes to the design that is still evolving at this writing. The differences were mainly contained in the divertor region as well as a small change to the top/bottom of the OB blanket to accommodate the wider divertor slot. The blanket, structural ring, and divertor are separated toroidally by 2 cm wide assembly gaps while the VV and LT shield are continuous toroidally. The torus was then divided into an upper half and a lower half. The difference between these two halves was in the blanket region behind the divertor support structure. In the upper half, the flat blanket has a composition identical to the IB breeding region (81.92% LiPb, 18.08% SiC whereas in the lower half it is composed of the LiPb manifolds and shield (30% LiPb, 60% SiC, 4% MF82H, 6% He). Figures 15 and 16 show the upper and lower models, respectively.

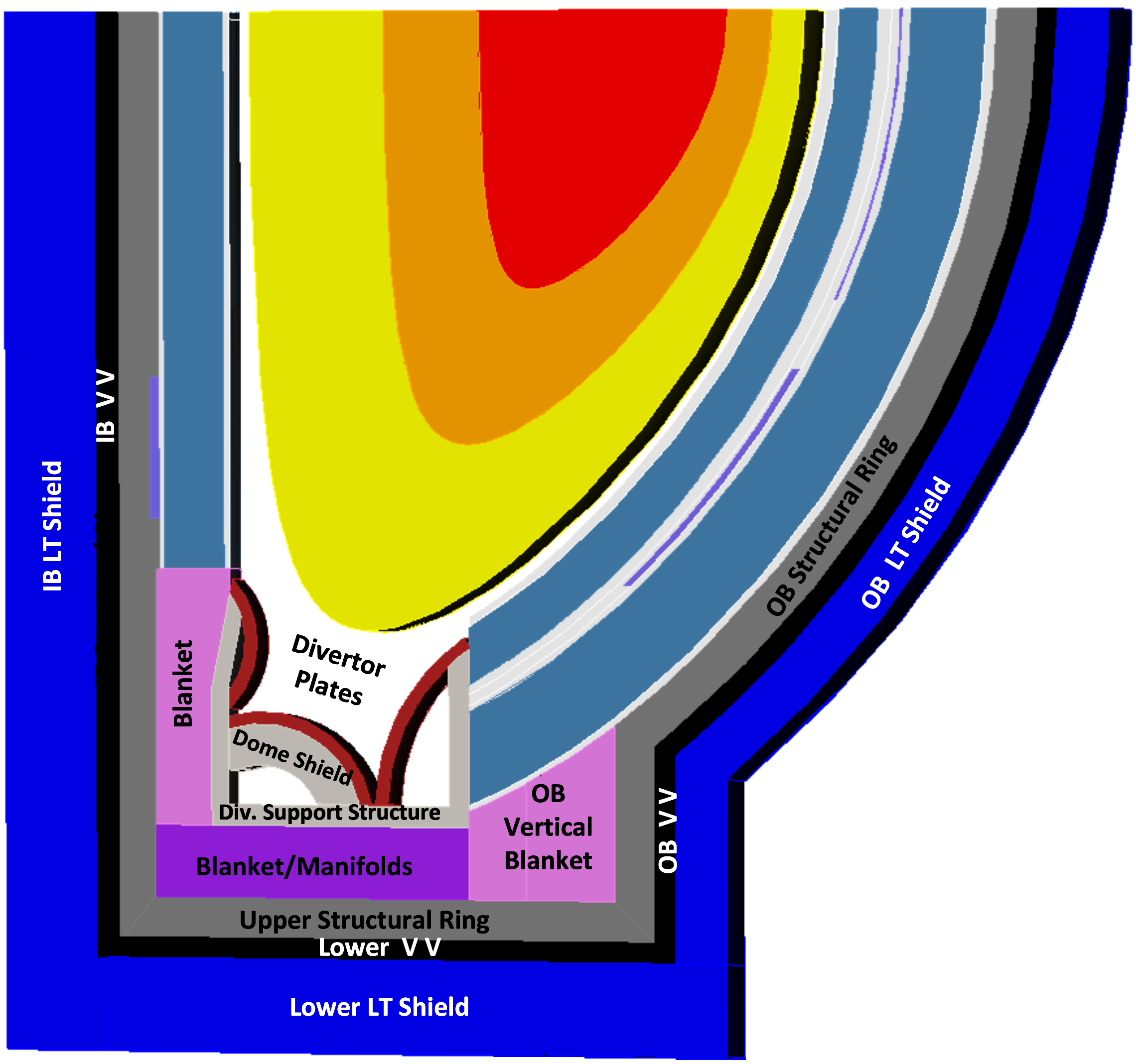

Fig. 16. Model of the lower half of the ARIES-ACT-1 design. The difference in the divertor region can be seen. The flat blanket below the divertor (purple) varies between this model and Figure 15.

V-b. 1/16th Module Nuclear Heating

This analysis modeled two separate entities: an upper 32nd and a lower 32nd. The upper and lower were then added together and multiplied by two to obtain one whole module (1/16th of the torus). This provided the heating in a single module. Table 3 gives a simple breakdown of the heating for a fusion power of 1804 MW and then a more detailed analysis is examined in Table 4. The heat deposited in the vacuum vessel and low-temperature (LT) shield are low-grade heat that will not be included in the power balance.

Table 3. Broad Breakdown of Nuclear Heating in 1/16th Module

Nuclear Heating (MW)	**Inboard**	**Outboard**	**Divertor**	**Total**
FW/Blanket	16.32	61.56	4.45	82.33
Divertor Plates, Support Structure, Dome Shield	---	---	11.10	11.10
Stabilizing Shells	0.51	2.83	---	3.34
Structural Ring	2.39	1.56	0.21	4.16
Total	19.22	65.95	15.76	100.92
Vacuum Vessel	0.88	0.42	0.07	1.37
LT Shield	3.22	1.29	0.14	4.65

Table 4. Detailed Breakdown of Nuclear Heating in 1/16th Module

Inboard Nuclear Heating (MW)	
IB Blanket:	16.34
Front Wall	1.13
Back Wall	0.21
Side Wall	2.20
LiPb Breeding Zones	12.80
4 cm VS Shell	0.51
IB Structural Ring	2.39
Total IB	19.24
IB Vacuum Vessel	0.88
LT Shield	3.22
Outboard Nuclear Heating (MW)	
OB-I Blanket:	44.11
Front Wall	3.53
Back Wall	0.89
Side Wall	4.87
LiPb Breeding Zones	34.42
OB-I Vertical Blanket	0.40
Stabilizing Shells:	
1 cm Kink Shell	0.81
4 cm VS Shells	2.02
OB-II Blanket:	17.44
Front Wall	1.06
Back Wall	0.24
Side Wall	2.21
LiPb Breeding Zones	13.54
OB-II Vertical Blanket	0.39
OB Structural Ring	1.56
Total	65.94
OB Vacuum Vessel	0.42
LT Shield	1.30
Divertor Nuclear Heating (MW)	
Upper Divertor:	
6 cm W-based Divertor Plates:	3.26
Inner Plate	0.74
Dome	1.20

Outer Plate	1.32
Divertor Dome Shield	0.95
Divertor Support Structure	1.30
Blanket	2.22
Upper Structural Ring	0.10
Total	7.83
Upper Vacuum Vessel	0.04
LT Shield	0.07
Lower Divertor:	
6 cm W-based Divertor Plates:	3.28
Inner Plate	0.75
Dome	1.21
Outer Plate	1.32
Divertor Dome Shield	0.96
Divertor Support Structure	1.35
Blanket/LiPb Manifold	2.23
Lower Structural Ring	0.11
Total	7.93
Lower Vacuum Vessel	0.03
LT Shield	0.07

V-c. Total Nuclear Heating and Energy Multiplication

To find the total nuclear heating, all the data were multiplied by 16 (see Table 5). Adding up all the individual section's heating results in 1614.72 MW. The IB, OB, and divertor regions generate 19%, 65%, and 16% of the heating, respectively. About 85% of the heating is deposited in the FW/blanket and stabilizing shells while the structural ring captures 4% of the heating. Dividing the total heating by the neutron power (1804 MW x 0.8), an energy multiplication of 1.12 was obtained.

Approximately 100 MW of heating is deposited in both VV and LT shield. This is a large amount of low-grade heat that will negatively impact the power balance. Our recommendation is to thicken the IB blanket and SR by 10 cm each to capture most of this heat. The final ARIES-ACT-1 design will reflect this change to the IB blanket and SR thicknesses.

Table 5. Broad Breakdown of Nuclear Heating in Full ARIES-ACT-1 Design

Nuclear Heating (MW)	**Inboard**	**Outboard**	**Divertor**	**Total**
FW/Blanket	261.12	984.96	71.20	1317.28
Divertor Plates, Support Structure, Dome Shield	---	---	177.60	177.60
Stabilizing Shells	8.16	45.28	---	53.44
Structural Ring	38.24	24.96	3.20	66.40
Total	307.52	1055.20	252.00	1614.72
Vacuum Vessel	14.08	6.72	1.12	21.92
LT Shield	51.52	20.64	2.24	74.40

V-d. Impact of Assembly Gaps

In order to reveal the effect of the assembly gap width on the heat deposited in the VV and LT shield, the above analysis (for 2 cm wide assembly gap - the nominal case) was repeated for 1 cm wide gap and no gap. The results show that the nuclear heating does go up as more heat is produced in the high-temperature components instead of the VV and LT shield, but this increase is not significant enough to greatly reduce the heat load to the VV and LT shield. The important parameters are summarized in Table 6 below.

Table 6. Impact of Assembly Gap Width on VV and LT Shield Heating

	2 cm gap	**1 cm gap**	**No gap**
Nuclear Heating in HT components [MW]	1614.72	1621.12	1624.48
Energy Multiplication	1.119	1.123	1.126
Vacuum Vessel	21.92	21.28	20.64
LT Shield [MW]	74.40	71.84	70.56
Low-grade heat in VV and LT Shield (% of Total Heating)	5.97%	5.7%	5.6%

V-e. Impact of Thickening IB Blanket and Structural Ring

It is desirable that the low-grade heat in the vacuum vessel and low-temperature shield be much lower than the current 5.5-6% range. In order to remedy this, the thickness of the inboard blanket was extended. In Cases 2 and 3, it was extended 5 cm and 10 cm, respectively. The results are summarized in Table 7 below. The low-grade heat dropped from 4.7% for Case 1 (Table 5) to about 4.1% for Case 2 and 3.6% for Case 3. Two more cases extend the structural ring by 10 cm and 15 cm. These cases show a very similar result and the low-grade heat drops to 3.7% and 3.4%. Case 6 examined extending the inboard blanket to 45 cm and the structural ring of the inboard, outboard, and divertor to 30 cm. This resulted in a low-grade heat percentage of 2.65%. Case 7 is identical to Case 6 except that the divertor SR was maintained at the original 20 cm thickness. Cases 6 and 7 are compared in Table 8. The final Case 7 is preferred over Case 6 due to the fact that there is minimal impact on the low-grade heating and the SR thickness is reduced at the top/bottom. This reduction in SR thickness saves money, allows more space at the top/bottom for other peripherals, and helps keep the original dimensions and locations of the outer legs of the TF magnet and maintenance port opening unchanged. A further breakdown looking at the changes between Cases 6 and 7 in the structural ring, vacuum vessel, and low-temperature shield can be seen in Table 9. A broader breakdown of the overall heating in all components is given in Table 10 for Case 7. The final ARIES-ACT-1 radial/vertical builds that reflect the latest changes to all components is displayed in Fig. 17.

Table 7. Impact of Extending the IB Blanket and Structural Ring on VV and LT Heating

Case	**1**	**2**	**3**	**4**	**5**
IB Blanket Thickness	**35 cm**	**40 cm**	**45 cm**	**35 cm**	**35 cm**
IB SR Thickness	**20 cm**	**20 cm**	**20 cm**	**30 cm**	**35 cm**
OB and Top/Bottom SR Thickness	**20 cm**	**20 cm**	**20 cm**	**20 cm**	**20 cm**
IB Components Nuclear Heating (MW):					
IB FW/Blanket	261.12	275.67	286.99	263.01	262.99
Stabilizing Shell	8.16	7.11	6.23	9.03	9.02
Structural Ring	38.24	31.34	25.50	52.02	59.03
Total IB Heating	307.52	314.12	318.72	324.06	331.04
OB and Divertor Heating	1307.2	1307.2	1307.2	1307.2	1307.2
Total Nuclear Heating	1614.72	1620.32	1625.92	1631.26	1638.24
Energy Multiplication	1.119	1.123	1.127	1.130	1.135
Total Thermal Power (Nuclear + Surface Heating (418))	2032.72	2038.32	2043.92	2049.3	2056.24
LT components Nuclear Heating* (MW):					
IB Vacuum Vessel	14.08 (0.7%)	11.64 (0.6%)	9.69 (0.5%)	10.16 (0.5%)	8.78 (0.4%)
IB LT Shield	51.52 (2.5%)	41.77 (2.0%)	34.08 (1.6%)	35.25 (1.7%)	31.35 (1.5%)
OB and Top/Bottom VV and LT Shield	30.72 (1.5%)	30.72 (1.5%)	30.72 (1.5%)	30.72 (1.5%)	30.72 (1.5%)
Total Low-Grade Heat	96.32 (4.7%)	84.13 (4.1%)	74.49 (3.6%)	76.13 (3.7%)	70.85 (3.4%)

* Value between parentheses is percentage of thermal power.

Table 8. Impact of Altering SR Thickness on VV and LT Heating

Case	**6**	**7**
IB Blanket Thickness	**45 cm**	**45 cm**
IB SR Thickness	**30 cm**	**30 cm**
OB SR Thickness	**30 cm**	**30 cm**
Top/Bottom SR Thickness	**30 cm**	**20 cm**
IB Components Nuclear Heating (MW):		
IB FW/Blanket	287.49	287.49
Stabilizing Shell	6.38	6.38
Structural Ring	36.71	36.71
Total IB Heating	330.58	330.58
OB and Divertor Heating	1321.29	1320.08
Total Nuclear Heating	1651.87	1650.66
Energy Multiplication	1.145	1.144
Total Thermal Power (Nuclear + Surface Heating (418))	2069.87	2068.66
LT components Nuclear Heating* (MW):		
IB Vacuum Vessel	6.71 (0.32%)	6.71 (0.32%)
IB LT Shield	24.96 (1.21%)	24.96 (1.21%)
OB and Top/Bottom VV and LT Shield	23.22 (1.12%)	23.46 (1.13%)
Total Low-Grade Heat	54.89 (2.65%)	55.13 (2.67%)

* Value between parentheses is percentage of thermal power.

Table 9. Breakdown of Heating Between SR, VV and LT Shield for Cases 6 and 7

Case	**6**	**7**
IB SR	36.71	36.71
Top SR	2.11	1.53
Bottom SR	2.30	1.67
OB SR	35.81	35.81
Total SR Heat	**76.93**	**75.72**
IB VV	6.71	6.71
Top/Bottom VV	0.98	1.12
OB VV	4.81	4.81
Total VV Heat	**12.50**	**12.64**
IB LT Shield	24.96	24.96
Top/Bottom LT Shield	2.14	2.24
OB LT Shield	15.29	15.29
Total LT Shield Heat	**42.39**	**42.49**

Table 10. Broad Breakdown of Nuclear Heating in Full ARIES-ACT-1 Design for Final Case 7

Nuclear Heating (MW)	**Inboard**	**Outboard**	**Divertor**	**Total**
FW/Blanket	287.49	985.30	74.02	1346.81
Divertor Plates, Support Structure, Dome Shield	---	---	176.20	176.20
Stabilizing Shells	6.38	45.55	---	51.93
Structural Ring	36.71	35.81	3.20	75.72
Total Recoverable Heat	330.58	1066.66	253.42	1650.66
Vacuum Vessel	6.71	4.81	1.12	12.64
LT Shield	24.96	15.29	2.24	42.49
Total Low-Grade Heat	31.67	20.1	3.36	55.13

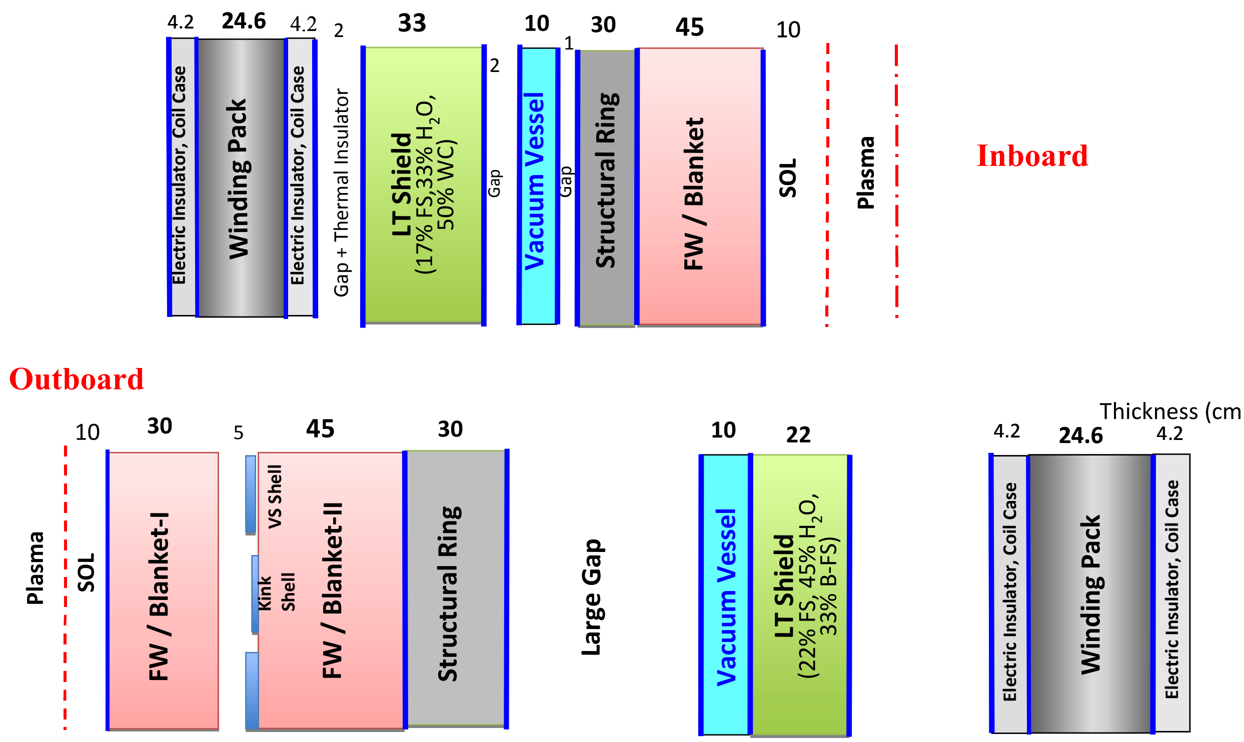

Fig. 17. Final ARIES-ACT-1 radial and vertical builds.

VI. Thermal Power Split Between He and LiPb Coolants

We evaluated the thermal heat loads to the helium and LiPb coolants for Case 7 with input from the July 2012 ARIES Systems Code Strawman on the surface heating and pumping power. The split between the He and LiPb loads is an essential parameter to the power conversion system and also to the ARIES Systems Code for the purpose of costing the He and LiPb heat transfer/transport system. The distribution of power is summarized in Table 11. Most of the divertor and blanket He and LiPb pumping powers are recovered by the helium and LiPb coolants as thermal power. The end result is 26:74 for the He:LiPb thermal power ratio.

Table 11. Thermal Power Split Between He and LiPb Coolants

Thermal Power (MW_{th})	**He**	**LiPb**	**Total**
Surface Heating	275*	130*	**405**
Recovered Power from Divertor Pumping	9*	---	**9**
Recovered Power from Blanket Pumping	---	4*	**4**
FW/Blanket, Manifolds, Stabilizing Shells#	---	1395.55	**1395.55**
Divertor Plates, Support Structure, Dome Shield	176.20	---	**176.20**
Structural Ring, ½ IB VS Shell	78.91	---	**78.91**
Total	**539.11** (26%)	**1529.55** (74%)	**2068.66**

* July 2012 ASC Strawman.

\# ½ IB VS shell, OB Kink shell, and OB VS shell.

VII. Conclusions

State-of-the-art tools were utilized to assess operational parameters of the ARIES-ACT-1 design. The DAGMC code was used to couple solid-modeling software with the MCNP Monte Carlo radiation transport code in order to effectively perform 3-D nuclear analysis on the tokamak geometry with fine details of various design elements of the blanket regions in particular. The results reveal that the ARIES-ACT-1 design satisfies the ARIES breeding requirements of 1.05 calculated TBR with ~50% ^{6}Li enrichment, energy multiplication of 1.144, and He:LiPb thermal power ratio of 26:74 .

Our recent nuclear heating analysis has reshaped the radial build in order to control the heat leakage to the low-temperature components and enhance the power balance. The total usable heat increased from 2033 MW to 2069 MW, which is a 1.8% increase and will, to a first order, decrease the cost of electricity by a comparable amount. Of course, the thicker IB blanket and SR will increase the capital and replacement costs but this could be offset by the corresponding decrease in the LT shield thickness needed to protect the magnets. Only a complete ARIES System Code run will verify our expectation. The level of low-grade waste heat around 2-3% is tolerable. Even though this heat is not available for energy conversion, it might be used for facility and hot water heating and could also be channeled through heat exchangers to provide clean heat.

Acknowledgment

This work was performed under the auspices of the US Department of Energy under contract #DE-FG02-98ER 54462.

References

1. The ARIES Project: http://aries.ucsd.edu/ARIES/.

2. F. NAJMABADI, A. ABDOU, L. BROMBERG, T. BROWN, V.C. CHAN, M.C. CHU, F. DAHLGREN, L. EL-GUEBALY et al., "The ARIES-AT Advanced Tokamak, Advanced Technology Fusion Power Plant," *Fusion Engineering and Design*, **80**, 3 (2006).

3. L.A. EL-GUEBALY, "Nuclear Performance Assessment of ARIES-AT," Fusion Engineering and Design, **80**, 99-110 (2006).

4. L. EL-GUEBALY, A. JABER, and S. MALANG, "State-of-the-Art 3-D Assessment of Elements Degrading the TBR of the ARIES DCLL Blanket," *Fusion Science and Technology* **61** (2012) 321-331.

5. L. EL-GUEBALY and S. MALANG, "Toward the Ultimate Goal of Tritium Self-Sufficiency: Technical Issues and Requirements Imposed on ARIES Advanced Fusion Power Plants," *Fusion Engineering and Design*, **84**, 2072 (2009).

6. "Cubit Geometry and Mesh Generation Toolkit version 12.2," Sandia National Laboratories (2010). Available at: http://cubit.sandia.gov.

7. "DAGMC Users Guide," University of Wisconsin-Madison Fusion Technology Institute (2008). Available at: http://cnerg.engr.wisc.edu/cgi-bin/index.cgi/wiki?p=DagmcUsersGuide.

8. X-5 Monte Carlo Team, "MCNP-A General Monte Carlo N-Particle Transport Code, Version 5," Vol. I, LA-UR-03-1987, Los Alamos National Laboratory (April 2003; revised 6/30/2004) and Vol. II, LA-CP-03-024S, Los Alamos National Laboratory (April 2003; revised 6/30/2004).

9. D.L. ALDAMA and A. TRKOV, "FENDL-2.1 Update of an Evaluated Nuclear Data Library for Fusion Applications," International Atomic Agency Report INDC(NDC)-467 (2004).

10. R.N. SLAYBAUGH, P.P.H. WILSON, L.A. EL-GUEBALY, and E.P. MARRIOTT, "Three-Dimensional Source Models for Toroidal Fusion Energy Systems," *Fusion Engineering and Design*, **84**, Issues 7-11, 1774 (2009)..

11. P. HUBBERSTEY, T. SAMPLE, and M. BARKER, "Is Pb-17Li Really the Eutectic Alloy? A Redetermination of the Lead-Rich Section of the Pb-Li Phase Diagram ($0.0 < x_{Li}$(at%) $<$ 22.1)," *Journal of Nuclear Materials*, **191-194**, 283 (1992).